

Dynamic behaviors of dust particles in the plasma–sheath boundary*

S. Takamura,^{†,a)} T. Misawa, and N. Ohno

Graduate School of Engineering, Nagoya University, Nagoya 464-8603, Japan

S. Nunomura

Department of Physics and Astronomy, The University of Iowa, Iowa City, Iowa 52242

M. Sawai and K. Asano

Graduate School of Engineering, Nagoya University, Nagoya 464-8603, Japan

P. K. Kaw

Institute of Plasma Research, Bhat, Gandhinagar, 382428, India

(Received 23 October 2000; accepted 28 December 2000)

A variety of dynamic behaviors in dusty plasmas is expected under the experimental condition of weak friction with gas molecules. The device “KAGEROU” provides such an environment for dynamic collective phenomena. Self-excited dust oscillations in Coulomb crystals have been observed at low values of plasma density and gas pressure. An instability mechanism was identified to be delayed charging in an inhomogeneous equilibrium dust charge in the sheath. The theoretical growth rate was formulated in relation to the destabilization of a transverse dust lattice wave (T-DLW), which was found to be very sensitive to the presence of a small amount of hot electrons which produces a substantial positive equilibrium charge gradient $\nabla Q_{d\text{-eq}}$ around the equilibrium position of dust particles in the plasma–sheath boundary. The first experimental observation of a correlated self-excited vertical oscillations in a one-dimensional dust chain indicates a destabilization of T-DLW. The experimental condition is very consistent with the parameter area which predicts numerically an instability of T-DLW. © 2001 American Institute of Physics.

[DOI: 10.1063/1.1350967]

I. INTRODUCTION

In a very low gas pressure, interesting dynamic behaviors of dust particles come out, although they are hidden in a high neutral density environment. Delayed charging gives us a new energy exchange process between the electric field and negatively charged dust particles traversing over an inhomogeneous equilibrium dust charge. The effect was first found experimentally in terms of spontaneous vertical oscillations of dust particles trapped at the plasma–sheath boundary.^{1,2}

In strongly coupled dust particles, unstable vertical motion of dust particles provokes a similar oscillation for neighboring particles, which makes a collective mode. One of them is the so-called transverse dust lattice wave (T-DLW). In a linear chain of dust particles, spontaneously excited T-DLW has been identified under a very low gas pressure.³ In a two-dimensional (2D) system, the transverse wave mode was also observed to be excited by applying the radiation pressure of laser light.⁴

In the present paper, we summarize the experiments on unstable vertical oscillations, especially the parameter-region which leads to the instability. The delayed charging is considered in the scheme of the dispersion relation for T-DLW including the stability of single particle motion. Depending on the condition, dust particles are either driven or braked

from the point of view of particle motion. In terms of wave motion, T-DLW is either destabilized or damped depending on the vertical gradient of equilibrium dust charge in a sheath, $\nabla Q_{d\text{-eq}}$. The growth rate is proportional to $\nabla Q_{d\text{-eq}}$ around the equilibrium floating position. The gradient is very sensitive to the sheath model. We will point out the importance of the electron energy distribution function, particularly the presence of suprathermal electrons.

The second topic is the first identification of spontaneously excited T-DLW in a linear chain of strongly coupled dust particles under a very low gas pressure condition.

In the next section, the observation of an unstable vertical oscillation will be represented with the parameter range which brings the unstable motion of particles. The effect of delayed charging on the dispersion relation of T-DLW, as well as the vertical oscillation of dust particles, will be discussed together with the plasma condition which leads to instability in the third section. In the fourth section we give the observation of spontaneously excited T-DLW. Finally, a discussion and a conclusion are given in the last section.

II. DYNAMICS OF PARTICLES

A variety of dynamic behaviors of dust particles appears under low gas pressure. Figure 1 shows several forces on dust particles as a function of particle radius under a typical glow discharge condition at $p = 100$ mTorr (Ar, $T_e \sim 1$ eV, $T_i \sim 0.1$ eV, $n_e = 10^{14}$ m⁻³, $\lambda_D \sim 500$ μ m, $\rho = 2.33$ g/cm³). The friction force with gas molecules f_n is comparable to the

*Paper MI 3.4, Bull. Am. Phys. Soc. **45**, 218 (2000).

[†]Invited speaker.

^{a)}Electronic mail: takamura@nuee.nagoya-u.ac.jp

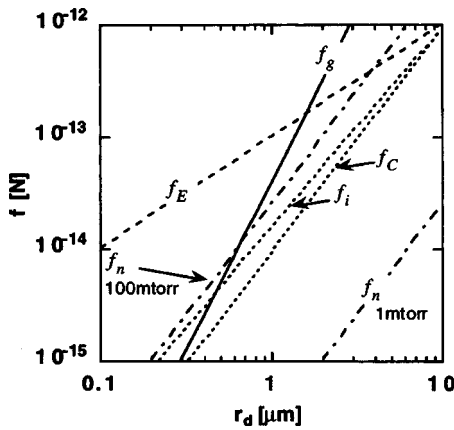


FIG. 1. Several forces on the dust particle trapped at the plasma–sheath boundary as a function of the particle radius under a typical glow discharge condition. (Ar, $p=100$ mTorr, $T_e=1$ eV, $T_i=0.1$ eV, $n_e=10^{14}$ m $^{-3}$, $\rho=2.33$ g/cm $^{-3}$, $\lambda_D\sim 500$ μ m.)

ion drag force f_i , the gravitational force f_g and the interparticle Coulomb force f_c . High neutral density in glow discharge is found to inhibit collective dynamic motions of dust particles, in particular, a rapid motion. However, the situation dramatically changes when the gas pressure reduces up to a few mTorr, as shown in Fig. 1. Recently, careful observations have been done in our group^{1–3,5} under very low gas pressures.

Experiments were performed in a dc Ar plasma device “KAGEROU” at a very low gas pressure less than 10 mTorr, generated by the dc discharge between hot filaments and the anodes, as shown in Fig. 2(a). The diffused plasma into the central area is confined by multiple cusps of the magnetic field generated with a series of permanent magnets. The typical experimental condition is summarized in Table I, in which we should note that the discharge voltage is as high as 70 V so that the energetic electrons may penetrate into the confined region under such a low gas pressure condition because of their long mean free-paths. Dust particles are trapped in a single horizontal layer in the plasma–sheath boundary area above a negatively biased mesh electrode. The biasing voltage is -10 V. These particles form a two-dimensional Coulomb crystal inside the ring electrode due to a strong repulsive Coulomb interactions as shown in Fig. 2(b). A He–Ne laser illuminates it. The particle behavior is observed with an intensified charge-coupled device (ICCD) camera system with the conventional speed of 30 frames/s.

The side view of a Coulomb crystal shows a vertically stable positioning of particles at the gas pressure of 4.4 mTorr in Fig. 2(c). When the pressure is decreased below a critical value, an instability arises and dust particles in the crystal oscillate spontaneously in the vertical direction, as shown in Fig. 2(d), in which a few images are superimposed for a period of 0.17 s. The vertical oscillation grows very slowly in time. A typical growth time is around 10 s. The dust happens to fall down from the trapping area when the amplitude exceeds around 2 mm. The FFT (Fast Fourier Transform) analyses give the frequency of 10–14 Hz. The total potential curve around an equilibrium position is approximated as a parabolic, giving an eigenfrequency of about

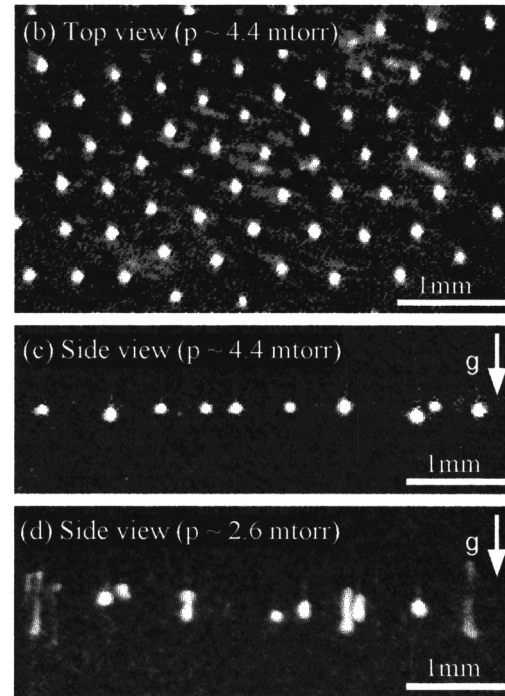
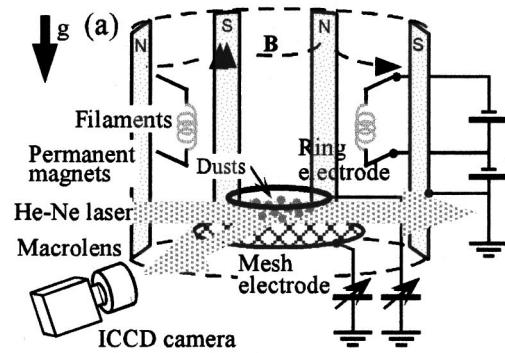


FIG. 2. (a) Schematic view of experimental device “KAGEROU.” (b) Top view of a two-dimensional Coulomb crystal in a high gas pressure. (c) Side view of the above crystal. (d) Side view of self-excited vertical oscillations of dust particles in a low gas pressure.

14 Hz, and a maximum amplitude of about 2.1 mm.¹ We should note that the equilibrium dust charge Q_d in the sheath changes the sign deep inside the sheath, causing a release of trapping.

TABLE I. Experimental condition and plasma parameters with dust particle characteristics.

| Parameters | Value |
|------------|--|
| I_d | 5–30 mA |
| V_d | 70 V |
| V_{ring} | -10 V |
| V_{mesh} | -5 – -60 V |
| P (Ar) | 2.0–4.0 mTorr |
| n_e | 10^{13} – 10^{15} m $^{-3}$ |
| T_e | 0.5–0.7 eV |
| V_s | $+1.3$ – $+2.0$ V |
| ρ | 1.2 or 1.5 g/cm 3 |
| r_d | 1.5 ± 0.25 , 2.5 ± 0.5 or 2.2 ± 0.05 μ m |

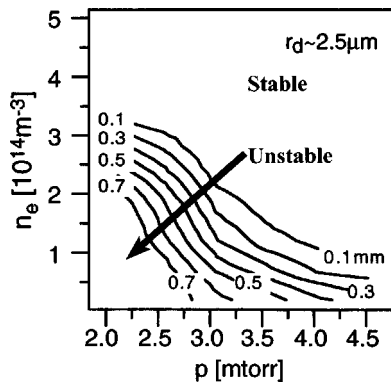


FIG. 3. Contours of the oscillation amplitude in the parameter space of n_e and p .

The spontaneous oscillation was observed either by decreasing the gas pressure or by decreasing the plasma density. It is summarized as a stability boundary close to 0.1 mm in amplitude in the n_e - p diagram of Fig. 3. It should be noted that particles are not levitable at very low plasma density so that the critical plasma density n_{ec} should be recognized.

We should consider the physical mechanism of energy supply against the dissipation due to friction with gas molecules. Delayed charging is pointed out to be a candidate for the energy gain from the sheath electrostatic field.⁶ The charging time $\partial Q/\partial I$ is generally very short, 35 μ s, for example, in the present case compared with the oscillation period of 67 ms. Nevertheless, it is still finite, not zero. The instantaneous charge on the dust is given by

$$Q_d(t) = Q_d(0) + \int_0^t (I_i + I_e) dt. \quad (1)$$

We can follow it during the movement of dust particles in the inhomogeneous sheath. The $Q_d(t)$ may differ from the equilibrium value Q_{d-eq} so that the dust may be either more accelerated and less decelerated or more decelerated and less accelerated on the way of periodic motion compared to that in the case of instantaneous charging. The acceleration is obtained on the part $\mathbf{E} \cdot \nabla Q_{d-eq} < 0$, while the particle coming into the deep inside of sheath is slowed down by the electrostatic field because of $\mathbf{E} \cdot \nabla Q_{d-eq} > 0$. The reason the reduction of plasma density destabilizes the dust particles comes from the increase in the charging time inversely proportioned to n_e . We will discuss the physical aspect of the instability in the general formalism related to the transverse wave in the next section.

By looking carefully at Fig. 2(d) again, we note that the oscillation amplitude differs among particles: several particles stay quiet at the same time. In addition, particles sometimes fall down from the trapping area. It is not reproduced by the above single-particle analysis. Since the particles in the dust crystal are coupled with a strong Coulomb interaction, the particles exchange their energy through such a collective coupling. Therefore, the kinetic energy of specified particles can be increased by an energy transfer through Coulomb interaction from neighboring particles. This is thought

to be one of reasons why particles drop down. The spatial variation of oscillation amplitude in the vertical directions implies the collective interaction among particles: excitation of T-DLW.² It will be discussed in the fourth section.

III. IMPACT OF DELAYED CHARGING ON T-DLW

We first derive the dispersion relation for T-DLW⁷ with the delayed charging by using a simplified model of 1-D dust particle chain.⁸ Consider the dust particles in equilibrium along a straight line at a regular interval d ; when the n -th dust particle is vertically displaced from its equilibrium position, it experiences restoring forces by interaction with its nearest neighbors through a Debye screened Coulomb force and through direct interaction with vertically varying background electric field E . If z_n denotes the vertical displacement of the n -th particle from the equilibrium height, we get the linearized equation of motion:

$$m \left(\frac{d^2 z_n}{dt^2} + \beta \frac{dz_n}{dt} \right) = -Q(z) \cdot \frac{dE}{dz} z_n + \delta Q_n \cdot E(z) + \alpha(d) \cdot (2z_n - z_{n+1} - z_{n-1}), \quad (2)$$

where

$$\alpha(d) = \frac{Q(z)^2}{4\pi\epsilon_0 d^3} \left(1 + \frac{d}{\lambda_D} \right) \exp\left(-\frac{d}{\lambda_D} \right) \quad (3)$$

is the coupling coefficient related to the screened interparticle potential. m is the mass of the dust particle, λ_D is the Debye length, $E(z)$ is the sheath electric field, and β is the coefficient related to the friction force between a dust particle and neutral gas molecules. $Q(z)$ is the equilibrium charge on the dust particles levitated at the equilibrium position z , and δQ_n is the charge deviation from Q associated with the delayed charging due to the finite charging time, and matches the inhomogeneous charge variation when the dust particle oscillates through the sheath. The time variation of δQ_n is described by the charging equation

$$\frac{\partial \delta Q_n}{\partial t} = -\frac{\delta Q_n}{\tau_c} + \frac{dQ}{dz} \frac{z_n}{\tau_c}, \quad (4)$$

where τ_c is the charging time for the dust particle. It shows that for instantaneous charging (τ_c tending to zero), $\delta Q_n = (dQ/dz) \cdot z_n$, i.e., the charge takes on a value determined by the instantaneous vertical position, as expected; on the other hand, if τ_c tends to infinity, δQ_n tends to zero and the charge retains its original value. For a typical T-DLW with finite $\omega\tau_c \ll 1$, we assume that z_n and δQ_n oscillate as $\exp(-i\omega t + inkd)$. Substituting them into Eqs. (2) and (4), we obtain the modified T-DLW dispersion relation with the effect of delayed charging,

$$\omega^2 + i\beta^* \omega = \omega_0^2 - \frac{\alpha(d)}{m} (2 - e^{ikd} - e^{-ikd}). \quad (5)$$

Here, ω_0 is the eigenfrequency given by

$$\omega_0^2 = \frac{1}{m} \frac{d}{dz} (Q \cdot E), \quad (6)$$

and β^* is the effective damping rate given by

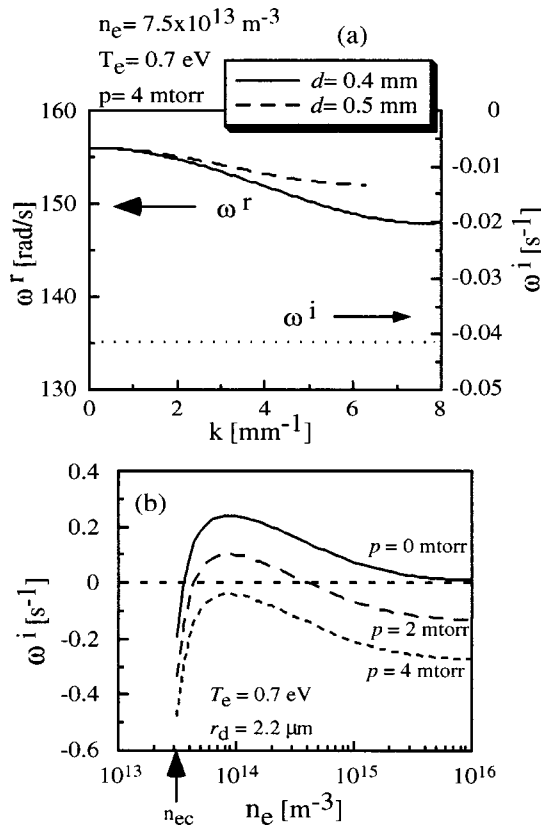


FIG. 4. (a) Dispersion relation for T-DLW under the close to experimental condition in the Child–Langmuir sheath model. $\omega = \omega^r + i\omega^i$. (b) Imaginary part of ω as a function of electron density taking gas pressure as a parameter.

$$\beta^* = \beta - 2\omega_i. \tag{7}$$

The effect of charging is represented by

$$\omega_i = -\frac{\tau_c}{2m} \frac{dQ}{dz} E. \tag{8}$$

It should be noted that the condition $\beta^* = 0$ gives a threshold condition for the instability of the T-DLW and provides a more general criterion corresponding to Eq. (6) in Ref. 1 for the dust particle instability. Note that ω_i represents the growth rate of the single dust particle oscillation at $\beta = 0$. Again the sign of $\mathbf{E} \cdot \nabla Q_{d-eq}$ is found to decide either driving or braking for a single particle motion.

Figure 4(a) shows an example of dispersion relation for T-DLW in our typical experimental condition. ω^r and ω^i are the real and imaginary parts of angular frequency, respectively. Nobody has yet succeeded in experimental verification of the propagation of T-DLW, although the propagation of L-DLW (Longitudinal Dust Lattice Wave) was clearly demonstrated in an rf discharge by Homman *et al.*⁹ Recently we succeeded in the observation of propagation of T-DLW externally excited and compared with the above theoretical dispersion relation.¹⁰

Figure 4(b) shows the imaginary part of the angular frequency, the growth rate, as a function of plasma density, taking a few gas pressure as a parameter. The condition $\omega^i > 0$ or $\beta^* < 0$ means the instability. We can distinguish that some stabilization appears just above the critical plasma den-

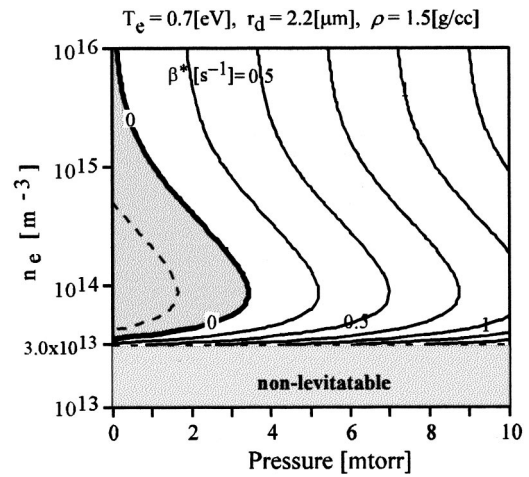


FIG. 5. Contour plot of $\beta^* = \beta - 2\omega_i$ in the parameter space of n_e and p . The area on the left side of $\beta^* = 0$ corresponds to the instability zone. The dust particle is nonlevitable at $n_e < n_{ec} = 3.0 \times 10^{13} \text{ m}^{-3}$.

sity n_{ec} below which the particles are nonlevitable. Instead, a destabilization or a weakening of damping appears over some range of plasma density. We note that ω^i approaches $\beta/2$ corresponding to no delayed charging in the high density limit, since τ_c approaches zero. The dispersion relation shown in Fig. 4 was obtained numerically using the Child–Langmuir sheath model. A similar stability boundary in the n_e - p diagram is shown in Fig. 5 taking β^* as a parameter. The left-hand area of the line $\beta^* = 0$ corresponds to an unstable zone. The critical plasma density for electrostatic levitation is found to be $3.0 \times 10^{13} \text{ m}^{-3}$. In the case of a Child–Langmuir sheath, we have a substantial ∇Q_{d-eq} so that the instability may be understood. However, the Child–Langmuir sheath model is a kind of approximation to a correct sheath structure. We can solve the Poisson equation with the boundary condition: the biasing voltage at the electrode and zero voltage at infinity corresponding to a plasma potential. The Poisson sheath gives so weak a ∇Q_{d-eq} that we may not expect any instability in the experimental condition, $T_e = 0.7 \text{ eV}$, as is indicated by a chain line (ratio=0%) in Fig. 6(a). We cannot expect any destabilization of T-DLW even higher T_e at the gas pressure in our experimental condition as shown in Fig. 7(a).

As is suggested in Sec. II, supra-thermal electrons may come into the dust trapping area because the discharge voltage is as high as 70 V and the gas pressure is so low that the mean free-path may be a device scale. Therefore, we assume a small amount of supra-thermal electrons although the Langmuir probe characteristic cannot distinguish their presence. A few percent of supra-thermal electrons dramatically change the equilibrium dust charge distribution in the sheath.

Again we employ Poisson equation to determine the sheath structure for two-component electrons, hot electrons with T_{eh} and cold ones with T_{ec} . Figure 6(a) shows the profiles of Q_{d-eq} in the sheath for some ratios of the hot electron population. We can distinguish the appearance of large ∇Q_{d-eq} for a plasma with a few percent of energetic electrons compared with a pure Maxwellian plasma. Figure 6(b) shows the stability boundary similar to Fig. 5 for the

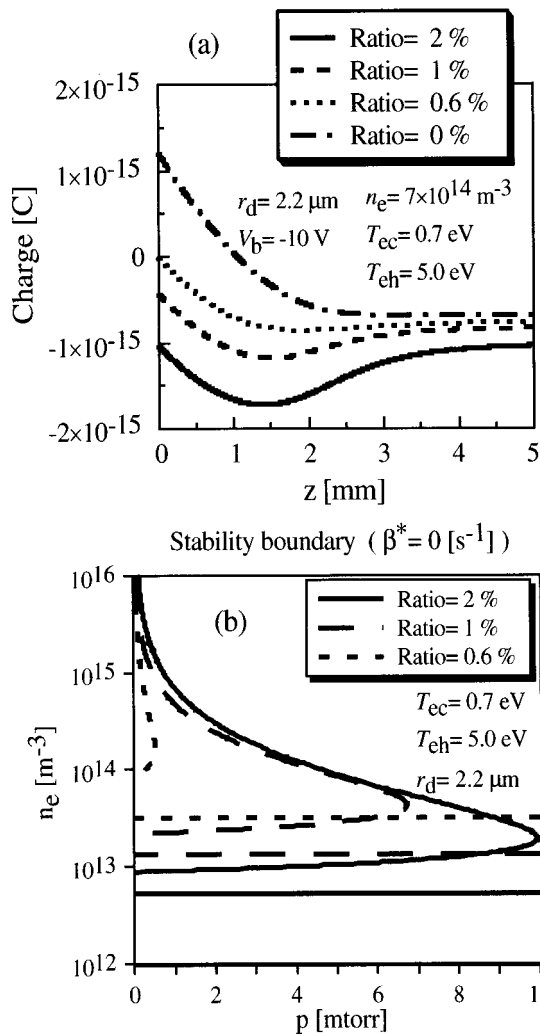


FIG. 6. (a) Equilibrium dust charge Q_{d-eq} as a function of height from the negatively biased electrode taking the ratio of the hot electron population as a parameter. (b) Stability boundary $\beta^* = 0$ in the parameter space of n_e and p taking the same quantity as a parameter.

Child–Langmuir sheath model. The boundary extends to high gas pressure for a small amount of hot electrons. Figures 7(b) and 7(c) give stability boundaries for $n_e - T_{eh}$ parameter space taking gas pressure as a parameter and for n_e -ratio of hot electron population parameter space, respectively. We understand reasonably well the destabilization of single particle, as well as T-DLW under our real experimental condition. The dust charge increases with the population of the hot electron so that the electrostatic upward force increases. However, it does not always mean an increase in destabilization because Q_{d-eq} distribution approaches again to that of pure Maxwellian plasma when the ratio increases. This is also suggested by Fig. 7(c).

The existence of hot electrons, which resolves the gap between experiments and the calculation, is attributed to the magnitude of the discharge voltage. There have been several papers in which the presence of hot electrons in similar devices is discussed.^{11,12} In addition, we have other evidence which supports our assumption. Figure 8 shows the eigenfrequency for vertical oscillations of dust particles in the sheath

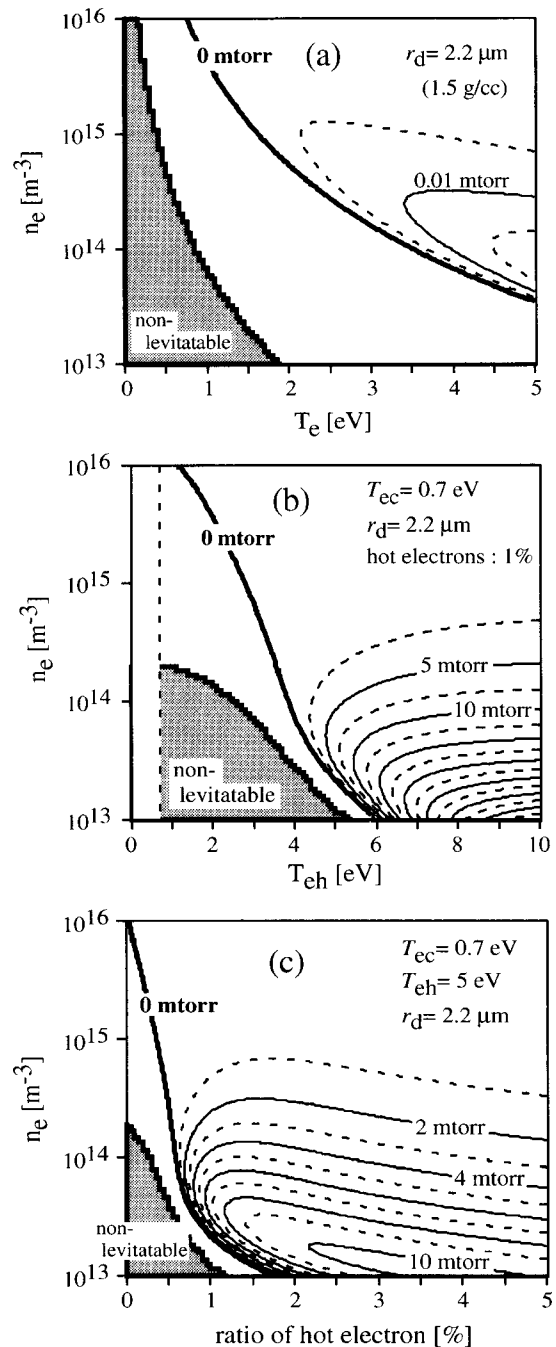


FIG. 7. (a) Stability boundary $\beta^* = 0$ in the parameter space of n_e and T_e for Maxwellian electrons taking the gas pressure as a parameter. (b), (c) Stability boundaries for non-Maxwellian electrons in the parameter spaces $n_e - T_{eh}$ and n_e -ratio of hot electrons, respectively.

potential well as a function of plasma density. The pure Maxwellian plasma with the observed T_e of 0.5 eV in this case cannot explain the dependence. Inclusion of a few percent of supra-thermal electrons reproduces very well the experimentally observed plasma density dependence of eigenfrequency. Experimental points were obtained by the observation of resonant excitation of vertical oscillation with a small external ac voltage on the biasing electrode. The equilibrium levitation height of dust particles is plotted in Fig. 9 as a function of again plasma density both with and without supra-thermal electrons. The presence of hot elec-

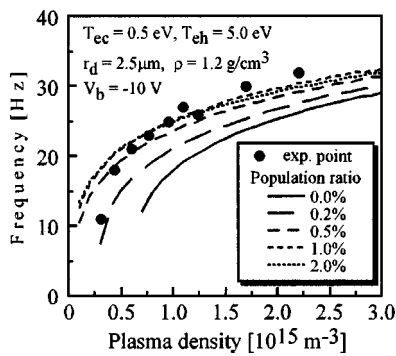


FIG. 8. Eigenfrequencies as a function of plasma density. Solid circles are experimental points. The sheath model without the electrons gives the theoretical curve with a solid line, while the models with some amount of hot electrons give dashed curves. The Ar gas pressure is about 4.0 mTorr except the lowest density case in which $P=2.0$ mTorr.

trons reproduces better the experimentally observed dependence than the sheath model without them although the effect is not so great.

IV. OBSERVATION OF SPONTANEOUSLY EXCITED T-DLW

In the second section, we described the instability of dust particles trapped at the plasma–sheath boundary in a low gas pressure. The origin of destabilization has been explained by the energy gain of dust particles with delayed charging from the sheath electric field. However, some of the oscillating particles were found to drop onto the electrode. In addition, an inhomogeneous vertical oscillation over the horizontal Coulomb lattice was also one of open questions.

The collective behaviors of the dusty plasma would be very important for explaining this discrepancy. The strong Coulomb coupling between neighboring particles allows the transverse wave to be excited in the Coulomb crystal. The standing wave formed by a superposition of the forward wave and backward wave reflected at the edge of the Coulomb crystal may enhance the vertical oscillations. Dust particles located deep in the sheath may have a positive charge or a weak upward force which would cause them to immediately fall.

In this section, we describe the first observation of self-excited transverse DLW propagating along a one-dimensional dust chain by observing the correlated motion of dust particles with a high speed ICCD camera system.¹³ The

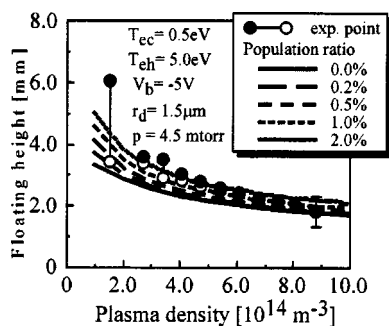


FIG. 9. Levitation height of dust particles as a function of plasma density.

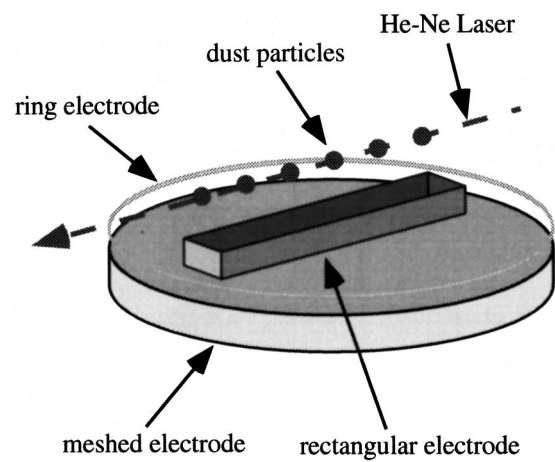


FIG. 10. Experimental configuration for forming a linear dust chain above a long rectangular box on a negatively biased mesh electrode.

experiments were performed again in a large unmagnetized plasma device ‘‘KAGEROU.’’ According to the previous numerical analysis on the dispersion relation of T-DLW, we chose the gas pressure as low as possible, 1.8 mTorr, and the plasma density as low as about $5 \times 10^{13} \text{ m}^{-3}$ in the plasma region. The electron temperature is found to be about 0.5 eV.

Dust particles can be levitated above a negatively biased meshed electrode and confined horizontally by a negatively biased ring electrode. A rectangular-shaped electrode on the biased mesh confines the one-dimensional chain of levitated dust particles as shown in Fig. 10. The bias voltage is about -10 V, and that of the ring electrode is about -50 V with respect to the grounded chamber. The diameter of the employed dust particles is $5 \pm 1 \mu\text{m}$. The high-speed ICCD camera system has a good temporal resolution with up to 125 image frames every second, that is, the sampling rate of this camera is 8 ms. Such a high temporal resolution is essential to analyze the dynamic behavior of the dust chain, because a

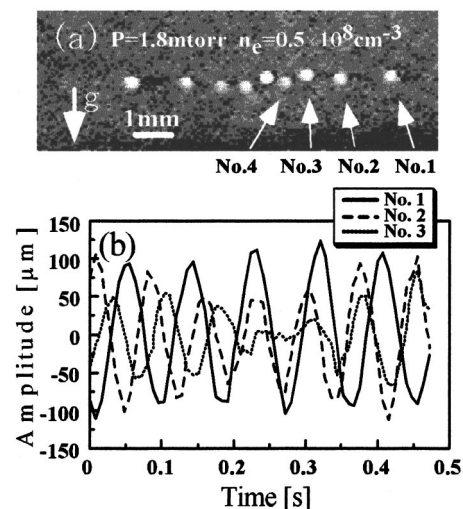


FIG. 11. (a) Typical snapshot taken by a high speed ICCD camera. (b) Time evolution of the vertical positions of the dust particles No. 1–3 for several periods.

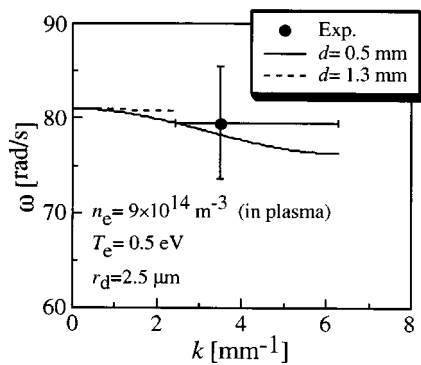


FIG. 12. Theoretical dispersion curve with an experimentally observed data point.

typical frequency of the self-excited vertical oscillation of dust particles is about 10–15 Hz.

Figure 11(a) shows a sample snapshot taken by this camera. It is found that nine dust particles almost aligned in a single row are trapped in the plasma–sheath boundary. The inter-particle distance d ranged from $0.5\text{--}1.3 \times 10^{-3}$ m. Figure 11(b) shows the time evolution of the vertical position of the particles No. 1–3 for several oscillation periods where we can observe a coherent wave motion. The FFT analysis reveals the oscillating frequency of about 12 Hz. A small deviation of the frequency influences the phase relation among dust particles oscillations over a very long period. This deviation, which may be due to a finite distribution of particle sizes, slightly complicates the phenomenon of T-DLW propagation.

Figure 12 shows the dispersion relationship calculated from Eq. (5) by taking the experimental conditions into account. The wavelength obtained from the time evolution of the levitated vertical positions of dust particles, and the frequency obtained by FFT analysis yield an experimental point on the ω - k space shown in Fig. 12. These experimental data are found to be in reasonable agreement with the theoretical curve of the T-DLW dispersion relation.

V. CONCLUSIONS

We observed self-excited vertical oscillations of dust particles in the Coulomb crystal at low values of plasma

density and gas pressure. An instability mechanism induced by delayed charging is proposed. Theoretical growth rate was formulated in relation to the destabilization of T-DLW.

The dispersion relation was studied carefully taking non-thermal energetic electrons into account. The effect of destabilization is found to be very sensitive to the presence of a small amount of hot electrons which produces a substantial $\nabla Q_{d\text{-eq}}$ around the equilibrium position of dust particles in the plasma–sheath boundary.

The first experimental observation of the self-excited vertical oscillation in a one-dimensional dust chain has been carried out at a very low gas pressure indicating the destabilization of T-DLW. The experimental condition is very consistent with the parameter area which predicts numerically an instability of T-DLW.

A key to observe the above dynamic behavior was found to be a deviation of electron energy distribution from a pure Maxwellian, especially the presence of a hot electron population.

- ¹S. Nunomura, T. Misawa, N. Ohno, and S. Takamura, *Phys. Rev. Lett.* **83**, 1970 (1999).
- ²S. Takamura, N. Ohno, S. Nunomura, T. Misawa, and K. Asano, in *Frontiers in Dusty Plasmas*, Proceedings of the 2nd International Conference on the Physics of Dusty Plasmas (Elsevier, Amsterdam, 2000), ICPDP-99, p. 337.
- ³T. Misawa, S. Nunomura, N. Ohno, and S. Takamura, *Jpn. J. Appl. Phys.* **39**, L551 (2000).
- ⁴S. Nunomura, D. Samsonov, and J. Goree, *Phys. Rev. Lett.* **84**, 5141 (2000).
- ⁵S. Nunomura, N. Ohno, and S. Takamura, *Phys. Plasmas* **5**, 3517 (1998).
- ⁶T. Nitter, T. K. Aslaksen, F. Melandso, and O. Havnes, *IEEE Trans. Plasma Sci.* **22**, 159 (1994).
- ⁷S. V. Vladimirov, P. Shevchenko, and N. F. Cramer, *Phys. Rev. E* **56**, R74 (1997).
- ⁸A. V. Ivlev, U. Konopka, and G. Morfill, *Phys. Rev. E* **62**, 2739 (2000).
- ⁹A. Homann, A. Melzer, S. Peter, and A. Piel, *Phys. Rev. E* **56**, 7138 (1997).
- ¹⁰T. Misawa, K. Asano, M. Sawai, N. Ohno, S. Takamura, and P. K. Kaw, *Phys. Rev. Lett.* **86**, 1219 (2001).
- ¹¹S. Robertson, *Phys. Plasmas* **2**, 2200 (1995).
- ¹²T. Yamazumi and S. Ikezawa, *Jpn. J. Appl. Phys.* **29**, 1807 (1990).
- ¹³T. Misawa, S. Nunomura, K. Asano, N. Ohno and S. Takamura, *T. IEE Japan* **120-A**, 180 (2000) (in Japanese).